

# Formation of Radical Anion Adducts between Dihydroxybenzenes and the Matrix Under Fast Atom Bombardment†

K. P. Madhusudanan\*

Medicinal Chemistry Division, Central Drug Research Institute, Lucknow-226 001, India

Dihydroxybenzenes give rise to anion radical adduct ions with 3-nitrobenzyl alcohol in addition to the deprotonated adduct ions under fast atom bombardment. 2-Nitrophenyl octyl ether gives only radical anion adducts, whereas other common matrices give deprotonated adducts. Unimolecular decomposition of  $[M + NBA - H]^-$  leads to both  $[M - H]^-$  and  $[NBA - H]^-$ , the abundances of which depend on the relative acidities of the dihydroxybenzenes. Similarly,  $[M + NBA]^{--}$  decomposes to  $[M]^{--}$  and  $[NBA]^{--}$ , the abundances of which reflect their relative electron affinities. Upon collision-induced decomposition,  $[M + NBA - H]^-$  gives mainly  $[M - H]^-$ , whereas  $[M + NBA]^{--}$  produces both  $[M - H]^-$ ,  $[M]^{--}$  and  $[NBA]^{--}$ . Higher radical anion clusters are also observed. Fast atom bombardment of the lithium-exchanged dihydroxybenzenes leads to similar radical anion adducts which decompose to give abundant ions corresponding to  $[M - H]^-$ ,  $[M + Li - 2H]^-$  and  $[M + Li - H + NO_2]^-$ . © 1998 John Wiley & Sons, Ltd.

*J. Mass Spectrom.* 33, 173–182 (1998)

**KEYWORDS:** radical anion adducts; dihydroxybenzenes; negative ion fast atom bombardment mass spectrometry; lithium exchange

## INTRODUCTION

In a previous paper,<sup>1</sup> we have shown the formation of radical anion adducts between paclitaxel and the matrix upon fast atom bombardment (FAB). Dihydroxybenzenes have been found to give abundant radical cation adducts under both FAB<sup>2</sup> and ammonia chemical ionization<sup>3</sup> conditions. There are several other examples of the formation of anomalous molecular ions under FAB,<sup>2</sup> but radical anion adducts are not commonly observed.  $\gamma$ -Cyclodextrin inclusion complexes of C<sub>60</sub> derivatives have been reported to give rise to radical anion adducts with the matrix.<sup>4</sup> Radical anion dimers have also been reported by Burinsky *et al.*,<sup>5</sup> and Cooks and co-workers.<sup>6</sup> Recently, Bruce and co-workers<sup>7</sup> have reported anion clustering of hydroquinone derivatives under negative ion chemical ionization (NICI) conditions. It was therefore of interest to study the negative ion FAB mass spectra of the isomeric dihydroxybenzenes to see whether these compounds also produce molecular anion adducts with matrix molecules.

## EXPERIMENTAL

The dihydroxybenzenes catechol (1), resorcinol (2) and hydroquinone (3) were commercially available samples

and used without any further purification. Their purity was checked by IR, NMR and mass spectral data. FAB mass spectra were recorded on a Jeol SX-102/DA-6000 double-focusing mass spectrometer with reverse geometry using a 6 kV xenon beam (10 mA). The matrices were obtained from Tokyo Kasei Kogyo (Tokyo, Japan). The FAB-desorbed ions were accelerated to 10 keV. The mass spectra were recorded by scanning the magnetic field over the mass range 0–2500 with a scan slope of 10 s and a cycle time of 12 s at a resolution of 3000. The samples were dissolved in methanol. Before recording the lithium-exchanged FAB mass spectra, the samples were prepared by adding LiOH to a methanolic solution of the dihydroxybenzenes and leaving it overnight. To record the D<sub>2</sub>O-exchanged spectra, D<sub>2</sub>O was added to the sample–matrix solution on the probe. This was repeated 2–3 times to achieve proper exchange.

Collision-induced dissociation (CID) mass spectra were recorded on the same instrument using the mass-analysed ion kinetic energy (MIKE) technique with a scan slope of 20 s and a cycle time of 25 s. Linked scans were also carried out to obtain neutral mass loss (at constant  $B/E(1 - E/E_0)^{1/2}$ ) and precursor ion (at constant  $B^2/E$ ) spectra. All the linked-scan and CID MIKE spectra reported here were recorded with helium in the collision cell. The pressure of helium (in the first field-free region collision cell for linked scan and in the second field-free region collision cell for CID MIKE) was adjusted so that the parent ion signal was reduced by 50%. Each linked scan and CID MIKE spectrum reported here is an average of 3–6 scans.

\* Correspondence to: K. P. Madhusudanan, Medicinal Chemistry Division, Central Drug Research Institute, Lucknow-226 001, India.

† CDRI Communication No. 5718.

## RESULTS AND DISCUSSION

The FAB mass spectra of the dihydroxybenzenes were recorded using different matrices such as glycerol, thioglycerol, 'magic bullet' (dithiothreitol–dithioerythritol (3:1)), 2-hydroxyethyl disulphide, sulpholane, 3-nitrobenzyl alcohol (NBA) and 2-nitrophenyl octyl ether (NPOE). However, only the nitro-containing matrices NBA and NPOE gave anion radical adduct ions; the others gave deprotonated adduct ions. The ion abundances in the negative ion FAB mass spectra of 1–3 recorded using NBA are given in Table 1. Dihydroxybenzenes are known to produce parent ions by hydroxyl group deprotonation under NICI conditions.<sup>8</sup> The negative ion FAB mass spectra also show abundant deprotonated molecular anions at  $m/z$  109. Further loss of a hydrogen radical leads to the formation of benzoquinone radical molecular ion. This ion at  $m/z$  108 is more abundant in hydroquinone, presumably owing to the higher stability of 1,4-benzoquinone having an electron affinity ( $EA$ ) of 177 kJ mol<sup>-1</sup>.<sup>9</sup> The adduct ion region shows peaks at  $m/z$  219 due to  $[2M - H]^-$ ,  $m/z$  262 and 263 corresponding to  $[M + NBA - H]^-$  and  $[M + NBA]^-$ , at  $m/z$  372 due to  $[2M + NBA - H]^-$ , at  $m/z$  415 and 416 due to  $[M + 2NBA - H]^-$  and  $[M + 2NBA]^-$ , at  $m/z$  525 due to  $[2M + 2NBA - H]^-$ , at  $m/z$  568 and 569 due to  $[M + 3NBA - H]^-$  and  $[M + 3NBA]^-$  and at  $m/z$  722 due to  $[M + 4NBA]^-$ . Even  $[M + 5NBA]^-$  at  $m/z$  875 could be detected. Catechol and resorcinol showed all these adduct ions, whereas hydroquinone gave predominantly the deprotonated adducts. The radical anion adducts were most prominent in catechol. In the D<sub>2</sub>O-exchanged spectra the  $m/z$  values are shifted as expected. For example, the peaks at  $m/z$  262 and 263 were shifted to  $m/z$  264 and 266, respectively, the peak at  $m/z$  372 was shifted to  $m/z$  376 and the peaks at  $m/z$  415 and 416 were shifted to  $m/z$  418 and 420, respectively.

The ion abundances in the negative ion FAB mass spectra of 1–3 recorded using NPOE are given in Table 2.  $[M + NPOE]^-$  is the only sample–matrix adduct

**Table 2.** Ion abundances in the negative ion FAB mass spectra of 1–3 using NPOE as the matrix

| Ion            | $m/z$ | 1   | 2   | 3   |
|----------------|-------|-----|-----|-----|
| $[M - 2H]^-$   | 108   | 29  | 24  | 100 |
| $[M - H]^-$    | 109   | 100 | 100 | 54  |
| $[M + NO_2]^-$ | 156   | 23  | 23  | 7   |
| $[2M - H]^-$   | 219   | 42  | 19  | 14  |
| $[M + NPOE]^-$ | 361   | 52  | 38  | 11  |

ion observed. The adduct ion is the most abundant in catechol and the least abundant in hydroquinone.  $[M - 2H]^-$ ,  $[M - H]^-$  and  $[2M - H]^-$  are the other characteristic ions from the dihydroxybenzenes. In hydroquinone, the base peak corresponds to 1,4-benzoquinone radical anion at  $m/z$  108. This observation suggests that the nitro group and the hydroxyl groups are essential for the formation of the radical anion adducts. In hydroquinone, because of the alternative pathway of easy oxidation to 1,4-benzoquinone, the radical anion adduct is not observed.

As the dihydroxybenzenes give abundant  $[M - H]^-$  ions under negative ion FAB conditions, addition of one or more molecules of matrix to  $[M - H]^-$  ions is probable. Association of another molecule of the dihydroxybenzene should give rise to  $[2M - H]^-$ . The formation of  $[2M - H + NBA]^-$  could be explained by the addition of NBA to  $[2M - H]^-$  ion. Since  $[NBA - H]^-$  ion is also prominent, addition of M and/or NBA to this ion can also result in some of these adduct ions. MIKE and CID MIKE spectra could confirm these different associations.

The  $[M + NBA - H]^-$  ions, on metastable decomposition, give rise to the deprotonated matrix and sample in different abundances (Fig. 1(a)–(c), Scheme 1). The  $[M - H]^-/[NBA - H]^-$  abundance ratios are 0.3 in 1, 0.6 in 2 and 5 in 3. This, in fact, reflects the proton affinity of the corresponding phenolate anion or the acidity of the phenol; the lower the ratio, the higher is the acidity.<sup>10</sup> The ratio decreases in the order  $3 > 2 > 1$ , whereas the gas-phase acidities increase in the order  $3 < 2 < 1$ .<sup>11</sup>

Upon CID, these adduct ions decompose mainly to  $[M - H]^-$  (Fig. 1(d)–(f)). The abundance of  $[NBA - H]^-$  is very small. The CID MIKE spectrum of the  $[Md_2 + NBAd_1 - D]^-$  ion at  $m/z$  264 [Fig. 1(g)] shows the expected  $[Md_2 - D]^-$  ion at  $m/z$  110. The ions due to NBA appear at  $m/z$  152 and 154, corresponding to  $[NBAd_1 - D]^-$  and  $[NBAd_1]^-$ , respectively. The latter ion could arise from a radical anion species of the same  $m/z$  value as shown in Scheme 2.

It may be noted that under FAB, abundant  $[NBA]^-$  ions are produced from NBA owing to its high  $EA$  of 88.7 kJ mol<sup>-1</sup>.<sup>12</sup> The observation of peaks corresponding to  $[M + NBA]^-$ ,  $[M + 2NBA]^-$ ,  $[M + 3NBA]^-$ ,  $[M + 4NBA]^-$  and  $[M + 5NBA]^-$  could be explained only on the basis of addition of neutral dihydroxybenzene to  $[NBA]^-$  followed by further addition of NBA. This is also indirectly supported by the absence of  $[2M]^-$  ions. In contrast to the reported radical anion clustering of hydroquinone derivatives,<sup>7</sup> radical anion adducts were the least abun-

**Table 1.** Ion abundances in the negative ion FAB mass spectra of 1–3 using NBA as the matrix

| Ion                 | $m/z$ | 1   | 2   | 3   |
|---------------------|-------|-----|-----|-----|
| $[M - 2H]^-$        | 108   | 30  | 40  | 100 |
| $[M - H]^-$         | 109   | 100 | 100 | 73  |
| $[M + NO_2]^-$      | 156   | 26  | 10  | 4   |
| $[2M - 3H]^-$       | 217   | —   | —   | 6   |
| $[2M - H]^-$        | 219   | 41  | 27  | 8   |
| $[M + NBA - 2H]^-$  | 261   | —   | —   | 17  |
| $[M + NBA - H]^-$   | 262   | 58  | 50  | 41  |
| $[M + NBA]^-$       | 263   | 91  | 29  | 9   |
| $[2M + NBA - H]^-$  | 372   | 4   | 7   | 2   |
| $[M + 2NBA - H]^-$  | 415   | 7   | 8   | 7   |
| $[M + 2NBA]^-$      | 416   | 16  | 11  | 2   |
| $[2M + 2NBA - H]^-$ | 525   | —   | 1   | 0.5 |
| $[M + 3NBA - H]^-$  | 568   | 1.4 | 0.6 | 0.5 |
| $[M + 3NBA]^-$      | 569   | 3   | 2   | —   |
| $[M + 4NBA - H]^-$  | 721   | —   | —   | 0.2 |
| $[M + 4NBA]^-$      | 722   | 0.7 | 0.5 | —   |

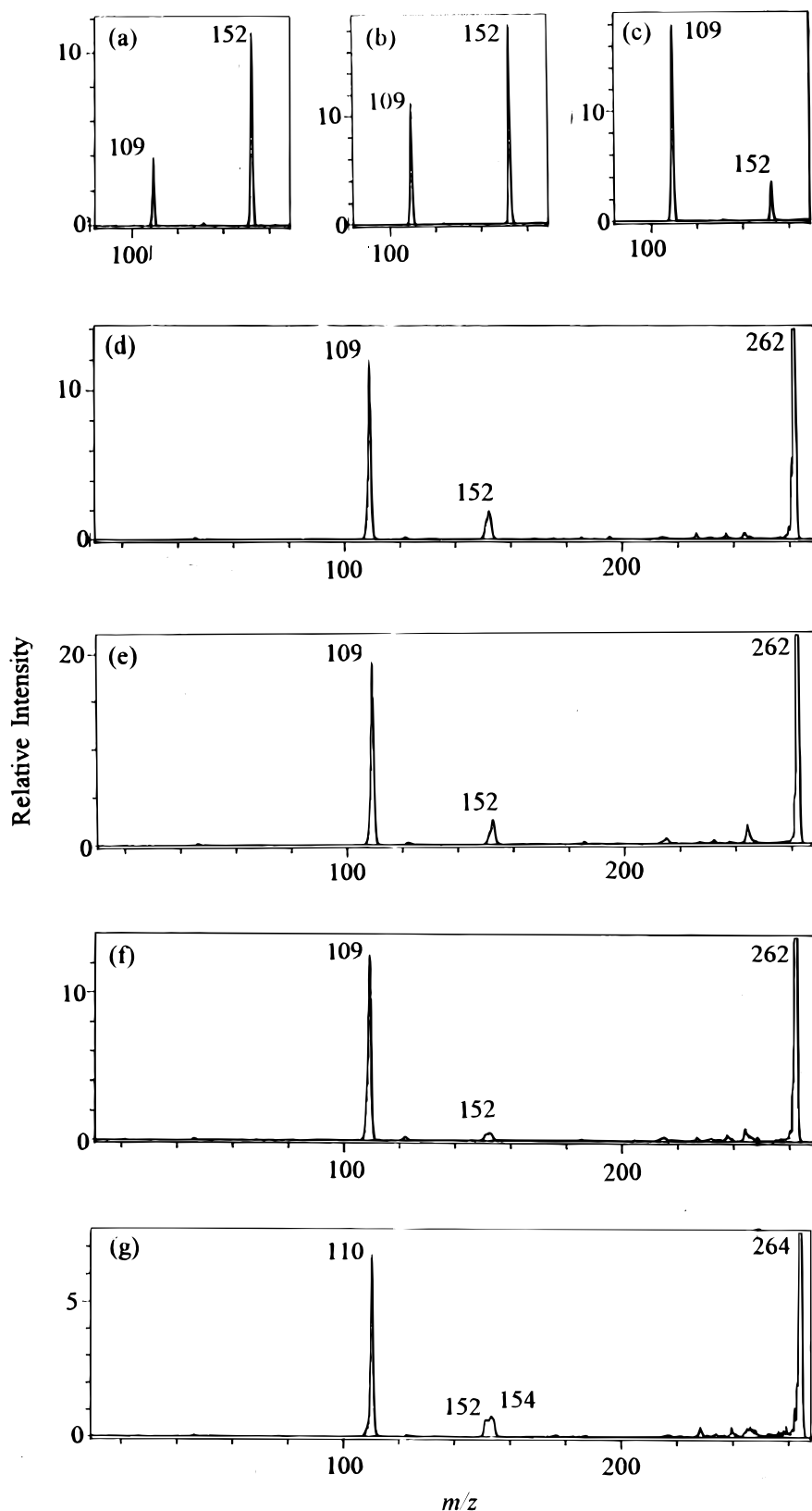
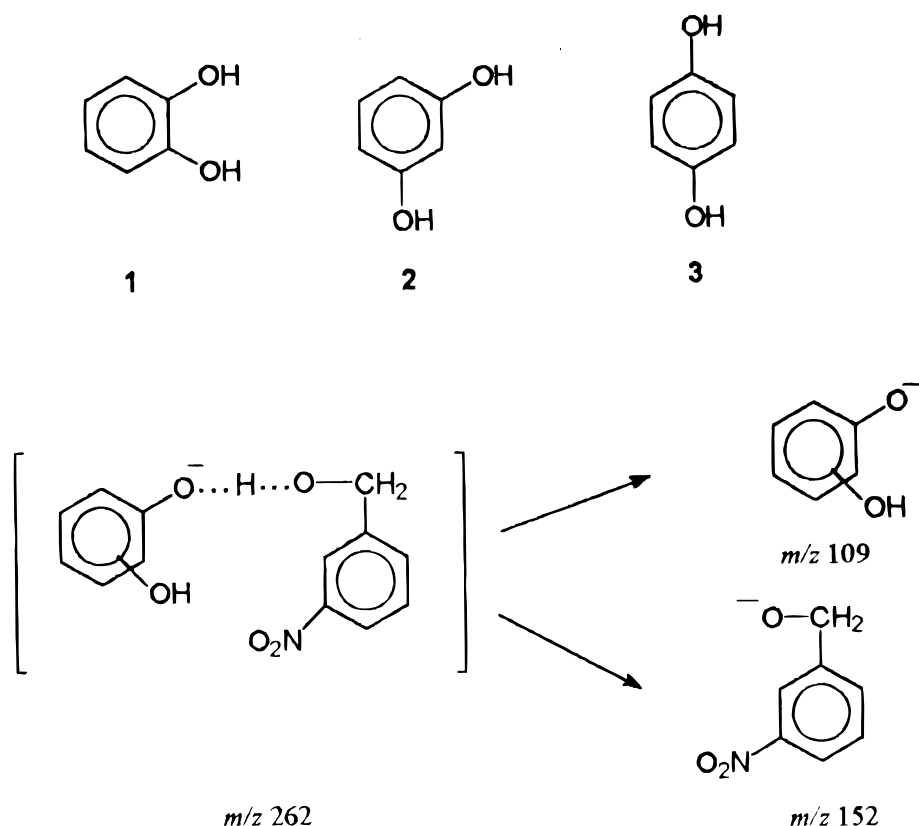


**Figure 1.** MIKE spectra of the  $[M + \text{NBA} - \text{H}]^-$  ions ( $m/z$  262) of (a) **1**, (b) **2** and (c) **3**, CID MIKE spectra of the  $[M + \text{NBA} - \text{H}]^-$  ions of (d) **1**, (e) **2** and (f) **3** and (g) CID MIKE spectrum of  $[\text{Md}_2 + \text{NBA} d_1 - \text{D}]^-$  of **1** ( $m/z$  264).

dant in hydroquinone under FAB. The association of neutral dihydroxybenzenes with the molecular anion of NBA could be proved by the MIKE spectra of these adduct ions. The MIKE and CID MIKE spectra of the

$[M + \text{NBA}]^{--}$  ions of **1–3** are shown in Fig. 2. It can be seen that these adduct ions decompose to  $[\text{NBA}]^{--}$  and  $[\text{M}]^{--}$  of the dihydroxybenzenes (Scheme 3). The  $[\text{M}]^{--}/[\text{NBA}]^{--}$  abundance ratio differs according to



Scheme 1

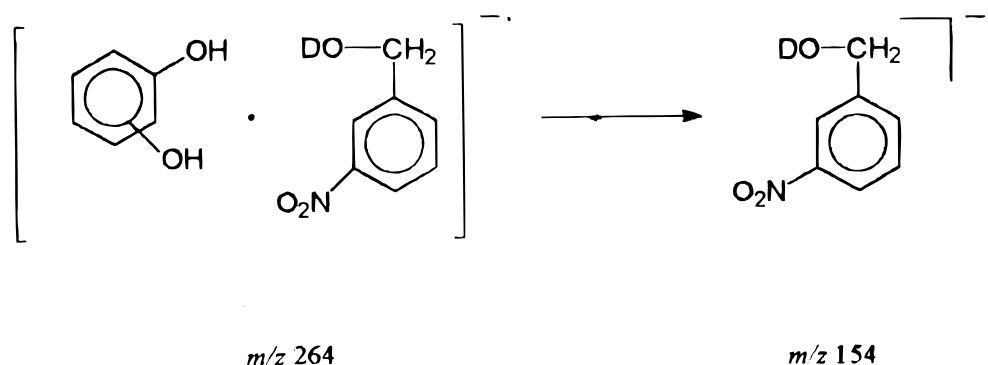
the substitution, being 0.2 in 1, 0.4 in 2 and 4 in 3. Burinsky *et al.*<sup>5</sup> and Cooks and co-workers<sup>6</sup> determined *EAs* by studying the dissociation of anion radical cluster ions. It was found that the natural logarithm of the abundance ratios correlated well with the *EAs* and that this method gives the relative orders of *EAs* of a series. From the spectra in Fig. 2(a)–(c) it appears that hydroquinone has the highest *EA* among the dihydroxybenzenes.

Collisional activation induces further fragmentation of  $[M]^{--}$  by loss of  $H^\bullet$  to give the stable  $[M - H]^-$  anion. This is evident in the CID MIKE spectra of the radical anion adducts given in Fig. 2(d)–(f). On closer examination, the peaks marked 109 are broad and also contain contributions from peaks at  $m/z$  110. The peaks are not resolved and it is difficult to assess the contribution from  $m/z$  110. The CID MIKE spectra of the corresponding deuterium-exchanged ion at  $m/z$  266, however, showed peaks at  $m/z$  110 and 112. As stated earlier, the matrix NPOE also gives rise to abundant  $[M$

+ NPOE] $^{--}$  adduct ions. This adduct ion from catechol upon CID decomposes to give  $[M - H]^-$  (6%) and  $[NPOE]^{--}$  (100%).

The CID MIKE spectra of the representative examples of the higher clusters of 1 are shown in Fig. 3. The  $[2M + NBA - H]^-$  ion at  $m/z$  372 shows a prominent loss of NBA and a minor loss of M [Fig. 3(a)]. Peaks are also observed corresponding to  $[M - H]^-$ , but NBA peaks are insignificant. Similar behaviour is also seen for  $[2M + 2NBA - H]^-$  at  $m/z$  525 (not shown) and  $[M + 2NBA - H]^-$  at  $m/z$  415 [Fig. 3(b)]. The  $[2M - H]^-$  ion at  $m/z$  219, as expected, decomposes to give  $[M - H]^-$  at  $m/z$  109 (not shown). These observations also indicate the formation of the deprotonated adduct ions by association of neutral molecules of M and/or NBA with the deprotonated dihydroxybenzene.

The radical anion adducts at  $m/z$  416 [Fig. 3(c)], 569, 722 [Fig. 3(d)] and 875 fragment predominantly by elimination of NBA, whereas loss of M is not significant and varies with the number of NBA molecules in the



Scheme 2

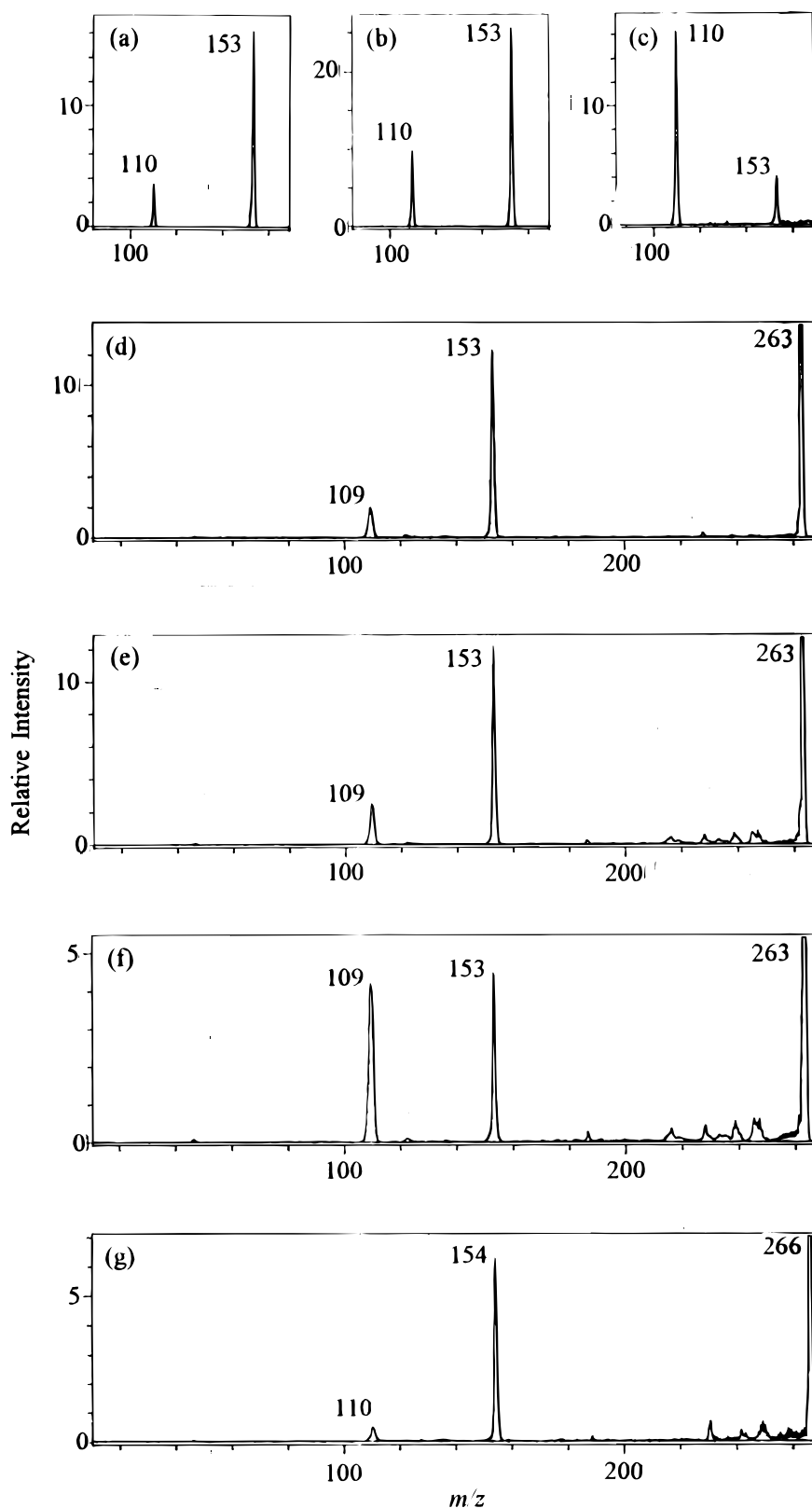
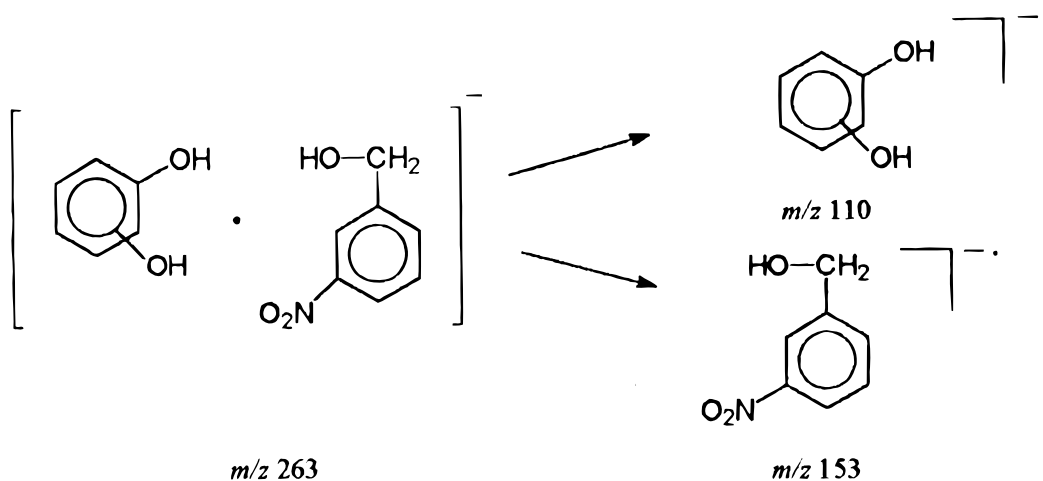


**Figure 2.** MIKE spectra of the  $[M + \text{NBA}]^{-}$  ions ( $m/z$  263) of (a) **1**, (b) **2** and (c) **3**, CID MIKE spectra of the  $[M + \text{NBA}]^{-}$  ions of (d) **1**, (e) **2** and (f) **3** and (g) CID MIKE spectrum of  $[\text{Md}_2 + \text{NBA}]^{-}$  of **1** ( $m/z$  266).

adduct. The  $[M + n\text{NBA} - \text{NBA}]^{-}/[M + n\text{NBA} - \text{M}]^{-}$  abundance ratio decreases as the value of  $n$  increases. For example, it is 14.4 for the adduct ion where  $n = 2$  but only 2 for the adduct ion where  $n = 5$ . Analogous differences in the

$[2M + n\text{NBA} - \text{H} - \text{NBA}]^{-}/[2M + n\text{NBA} - \text{H} - \text{M}]^{-}$  abundance ratio are also noted for the deprotonated adduct ions. Apparently, the cluster ions are more stabilized by H-bond interactions among NBA molecules as the number of NBA in the cluster increases. Unlike



Scheme 3

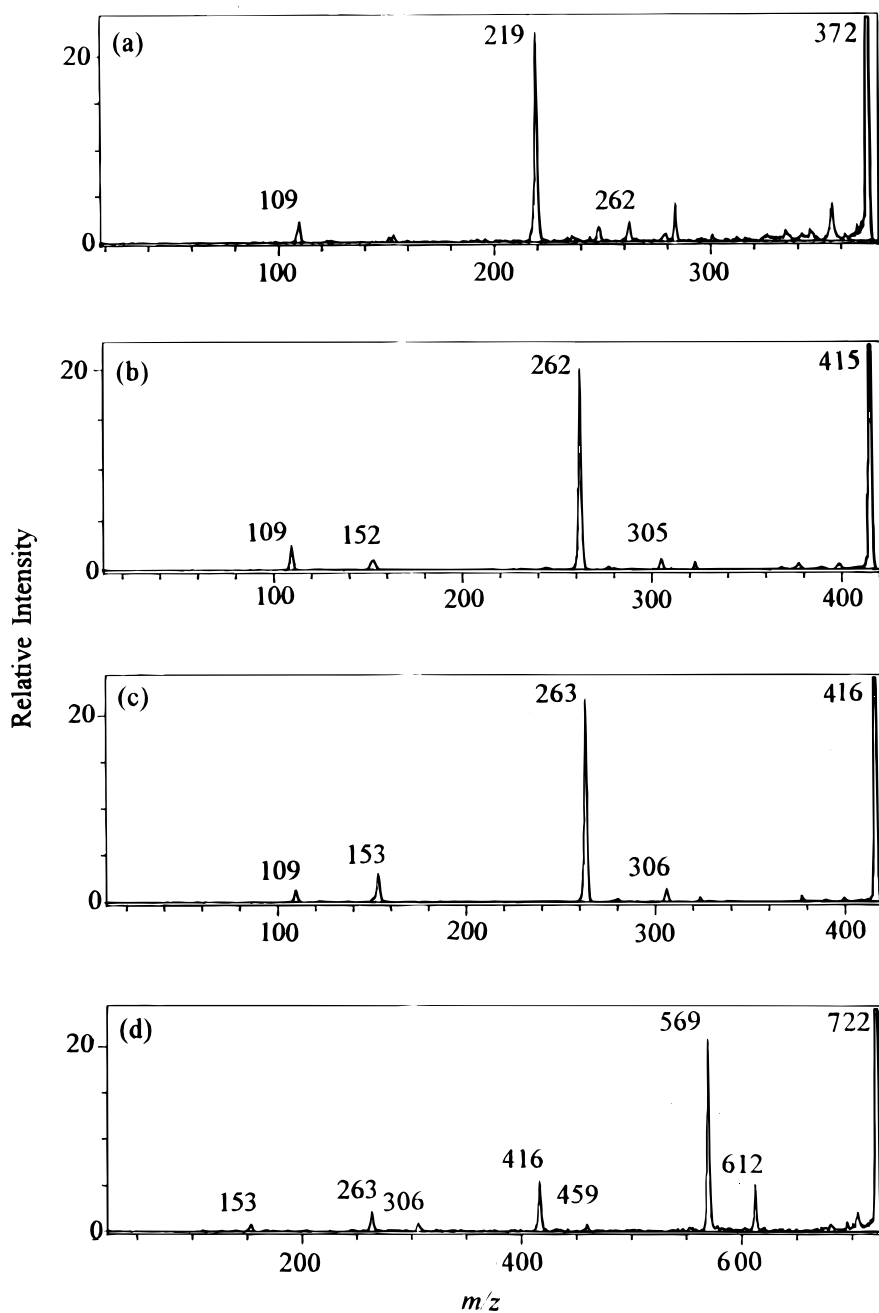


**Figure 3.** CID MS/MS spectra of cluster ions of **1**: (a)  $[2M + NBA - H]^+$  at  $m/z$  372, (b)  $[M + 2NBA - H]^+$  at  $m/z$  415, (c)  $[M + 2NBA]^+$  at  $m/z$  416 and (d)  $[M + 4NBA]^+$  at  $m/z$  722.

**Table 3.** Ion abundances in the negative ion FAB mass spectra of lithium-exchanged dihydroxybenzenes using NBA as the matrix

| Ion   | <i>m/z</i> | 1   | 2   | 3   |
|---|------------|-----|-----|-----|
| [M - 2H] <sup>-•</sup>                        | 108        | 24  | 40  | 100 |
| [M - H] <sup>-</sup>                          | 109        | 100 | 100 | 40  |
| [M + Li - 2H + NO <sub>2</sub> ] <sup>-</sup> | 161        | 11  | 12  | 29  |
| [M + Li - H + NO <sub>2</sub> ] <sup>-</sup>  | 162        | 33  | 46  | 34  |
| [2M - H] <sup>-</sup>                         | 219        | 19  | 10  | 4   |
| [2M + Li - 2H] <sup>-</sup>                   | 225        | 31  | 60  | 18  |
| [2M + 2Li - 3H] <sup>-</sup>                  | 231        | 14  | 13  | —   |
| [2M + 3Li - 4H] <sup>-</sup>                  | 237        | 17  | 13  | —   |
| [M + Li - 2H + NBA] <sup>-</sup>              | 268        | 20  | 25  | 58  |
| [M + Li - H + NBA] <sup>-•</sup>              | 269        | 43  | 55  | 36  |
| [M + 2Li - 2H + NBA] <sup>-•</sup>            | 275        | 11  | 2   | —   |

the deprotonated adduct ions, the radical anion adducts show peaks at *m/z* values corresponding to [*n*NBA]<sup>-•</sup> ions. These observations also corroborate the assumption that the deprotonated adduct clusters are formed by solvation of neutral molecules of M or NBA to the deprotonated M, whereas the radical anion adducts result from solvation of neutral M and/or NBA to the radical anion of NBA. As suggested by Bruce and co-workers,<sup>7</sup> a face-to-face approach of the neutral and ionic species could result in association via electron sharing between the components and by H-bonding with the hydroxyl groups. Recently, Wakisaka and co-workers<sup>13</sup> have reported mass spectral studies of molecular self-assembly involving non-covalent interactions between phenols and bases such as pyridine. It is possible that the NBA-dihydroxybenzene system may also be involved in such self-assemblies having interactions of OH and nitro groups.

We reported earlier that these dihydroxybenzenes give rise to radical cation adducts following lithium cationization.<sup>2</sup> The negative ion FAB mass spectra of 1–3 mixed with LiOH recorded using NBA showed radical anion adducts containing lithium (Table 3). The only previous report of the formation of metal-containing radical anions is that of metal carboxylate radical anions.<sup>14</sup> In the case of dihydroxybenzenes, as observed earlier,<sup>2</sup> hydroquinone behaved differently to resorcinol and catechol. Whereas the last two compounds gave abundant radical anion adducts with NBA in which either one (*m/z* 269) or both (*m/z* 275) of the hydroxyl hydrogens have been replaced with lithium, hydroquinone gave an abundant adduct of its [M + Li - 2H]<sup>-</sup> ion with NBA at *m/z* 268. [2M + *n*Li - (*n* + 1)H]<sup>-</sup> ions (where *n* = 1–3) are also abundant in the spectra of these compounds.

The CID/MS spectra of these lithiated adduct ions are shown in Fig. 4. The spectrum of the dilithiated (*m/z* 275) adduct ion of 1 displayed in Fig. 4(a) shows elimination of H<sub>2</sub>O and LiOH. The monolithiated radical anion adduct ion at *m/z* 269 [Fig. 4(b)] also shows loss of H<sub>2</sub>O. Peaks corresponding to [NBA]<sup>-•</sup> or [NBA - H]<sup>-</sup> are insignificant, whereas [M - H]<sup>-</sup> and [M + Li - 2H]<sup>-</sup> ions are fairly abundant. The peaks at *m/z* 162 from the monolithiated and at *m/z* 168 from the dilithiated adducts correspond to an unusual fragmentation resulting in ions that can be represented as

NO<sub>2</sub><sup>-</sup> adducts of mono- or dilithiated dihydroxybenzene, [M + Li - H + NO<sub>2</sub>]<sup>-</sup> or [M + 2Li - 2H + NO<sub>2</sub>]<sup>-</sup> (Scheme 4). The CID/MS spectrum of the deuterium-exchanged monolithiated catechol adduct at *m/z* 271 [Fig. 4(f)] shows that the ion at *m/z* 162 is shifted to *m/z* 163 and the phenolate anion is shifted to *m/z* 110 as expected. The [M + NBA + <sup>6</sup>Li - H]<sup>-•</sup> ion at *m/z* 268 [Fig. 4(g)] decomposes to give the ions at *m/z* 109, 114 and 161, thereby showing the presence of one lithium atom and a replaceable hydrogen in the ion at *m/z* 162. The direct formation of the ion at *m/z* 162 from [M + NBA + Li - H]<sup>-•</sup> is confirmed by precursor ion analysis (*B*<sup>2</sup>/*E* scan). A constant neutral mass-loss scan also showed the formation of the ions at *m/z* 162 and 168. This suggests a strong interaction between the NO<sub>2</sub> group and Li in these adducts. The CID of the deprotonated and lithiated adduct ions at *m/z* 268 leads to different abundances of [M - H]<sup>-</sup>, [M + Li - 2H]<sup>-</sup> and [M + Li - H + NO<sub>2</sub>]<sup>-</sup> (Scheme 5). In 1 the [M + Li - 2H]<sup>-</sup> ion at *m/z* 115 is prominent [Fig. 4(c)], presumably owing to the internal lithium bonding interactions. In 2 the [M + Li - H + NO<sub>2</sub>]<sup>-</sup> adduct ion assumes importance [Fig. 4(e)]. A hydrogen migration from OH of NBA to M appears to be favoured, resulting in this ion at *m/z* 162. The lithiated hydroquinone which showed only deprotonated and lithiated adduct ions at *m/z* 268 fragments to give abundant ions at *m/z* 108 and 161 (Fig. 4(d), Scheme 6). The stability of 1,4-benzoquinone appears to be the driving force for these reactions. The ion at *m/z* 161, as expected, generates an abundant ion at *m/z* 108 during CID.

Upon collisional activation, the [M + Li - H + NO<sub>2</sub>]<sup>-</sup> ion at *m/z* 162 decomposes mainly by loss of LiNO<sub>2</sub> to give the phenolate anion, apart from a small loss of HNO<sub>2</sub> to give the ion at *m/z* 115 [Fig. 5(a)]. Elimination of LiNO<sub>2</sub> has been reported earlier to occur from lithiated benzenes<sup>15</sup> and lithiated nitrostyrenes.<sup>16</sup> The deuterium-exchanged ion at *m/z* 163 correspondingly gives rise to the phenolate ion at *m/z* 110 [Fig. 5(b)]. Analogous fragmentation by loss of HNO<sub>2</sub> is observed during collisional activation of the [M + NO<sub>2</sub>]<sup>-</sup> ion of 1 at *m/z* 156 [Fig. 5(c)]. It may be of interest that the [M + Li - H + NPOE]<sup>-•</sup> ion at *m/z* 367 also yields the ion at *m/z* 162 during CID. This reaction seems to be a characteristic of the interactions between Li and nitro compounds.

In conclusion, it is clear that the nitro group in the matrix is responsible for the observation of radical anion clusters. It appears that the hydroxyl hydrogens of the dihydroxybenzenes are involved in H-bonding with the charged nitro group. The deprotonated adducts are observed only when the matrix has a hydroxyl group (as in NBA), which can undergo an H-bonding interaction with the [M - H]<sup>-</sup> ion of the dihydroxybenzene. This explains why [M + NPOE - H]<sup>-</sup> is not observed.

#### Acknowledgement

Grateful acknowledgement is made to the Regional Sophisticated Instrumentation Centre where the mass spectral studies were carried out.

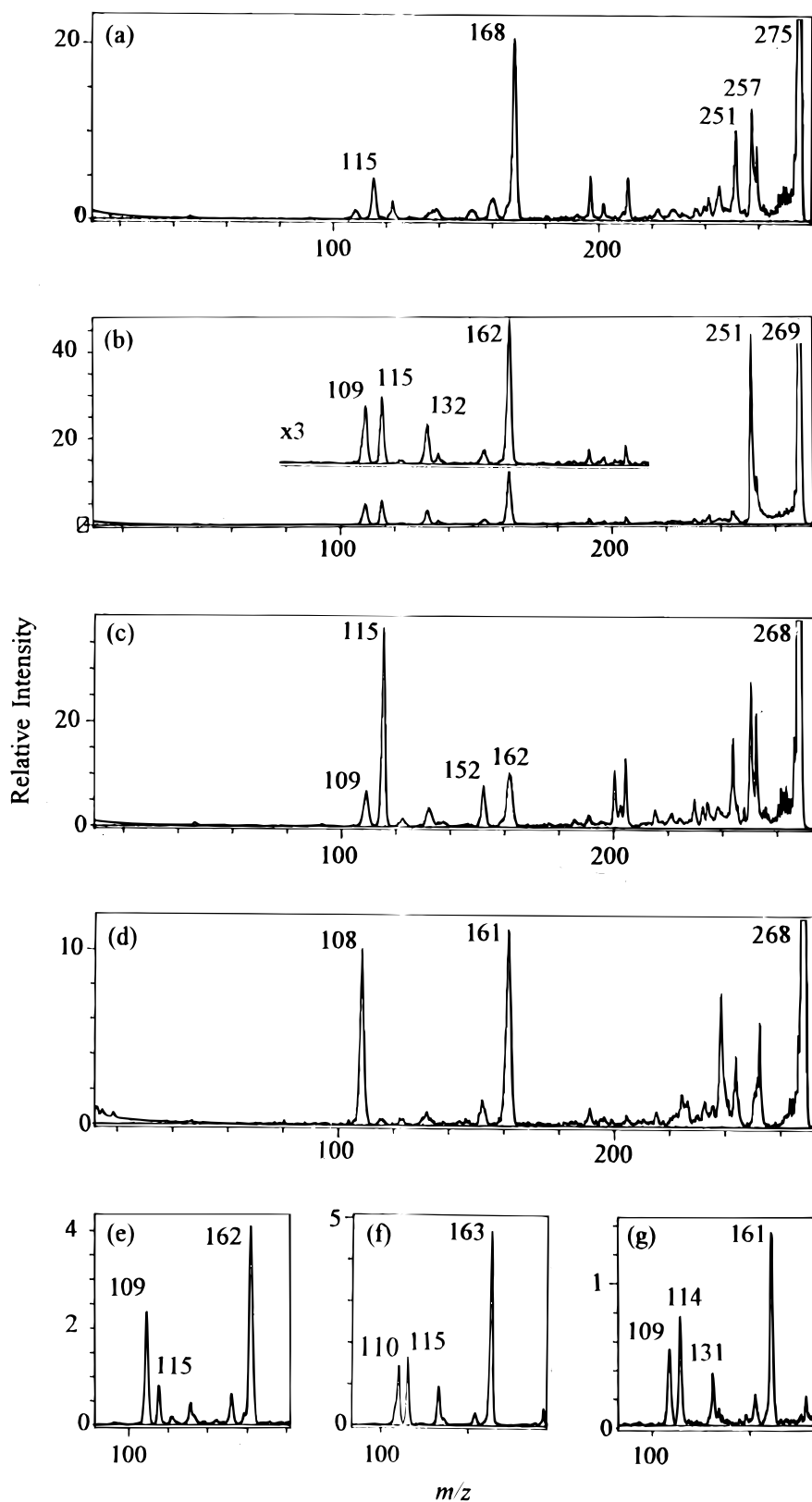
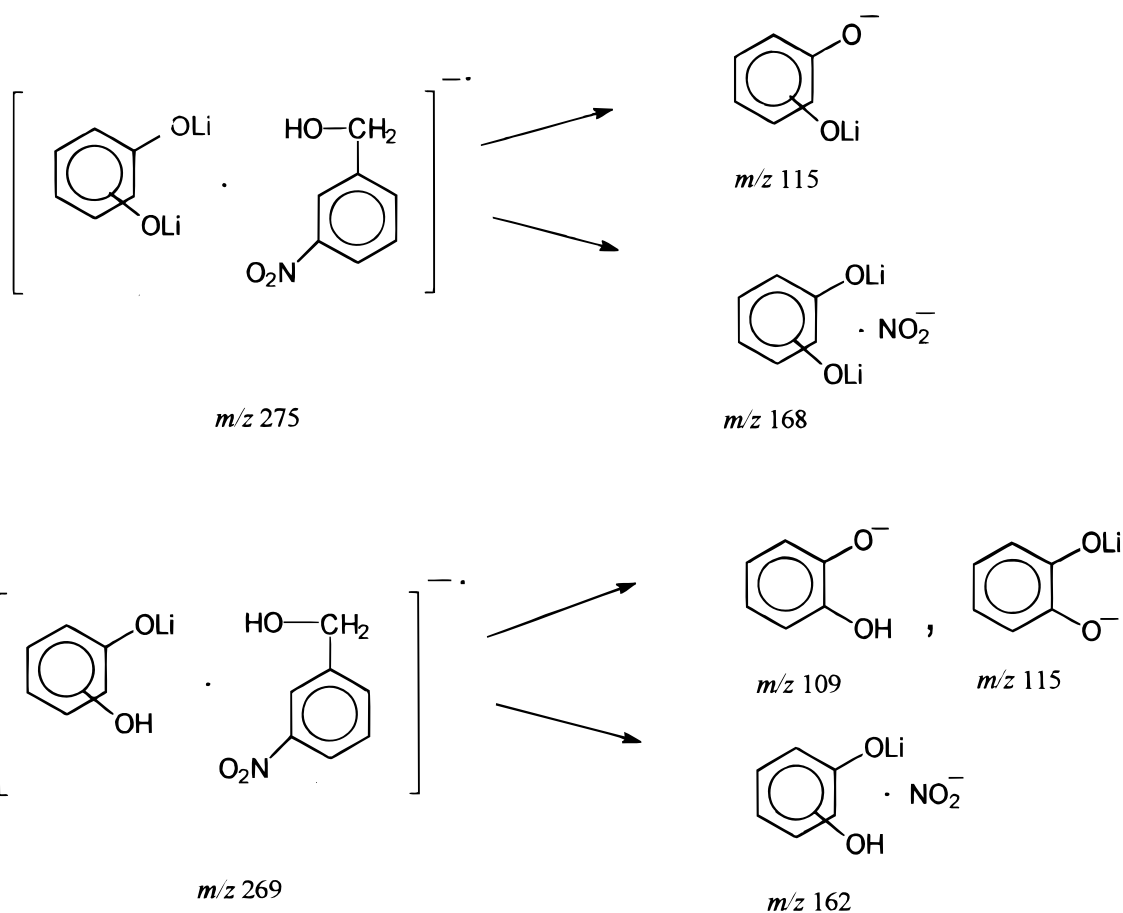
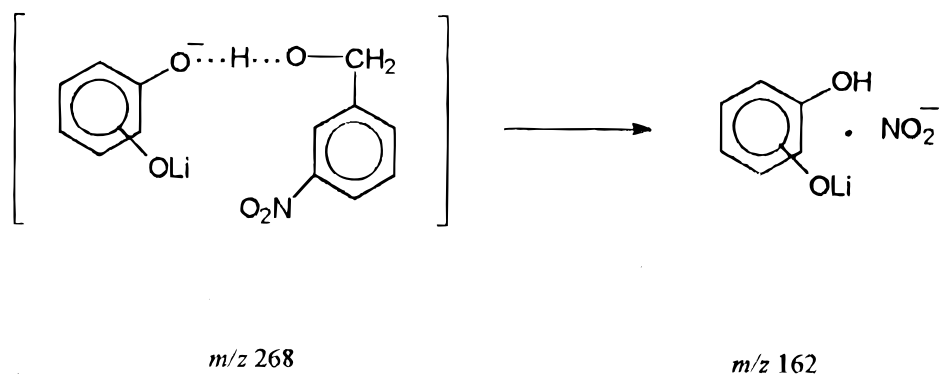


**Figure 4.** CID MIKE spectra of lithiated cluster ions (a)  $[M + 2\text{Li} + \text{NBA} - 2\text{H}]^-$  of **1** at  $m/z$  275, (b)  $[M + \text{Li} + \text{NBA} - \text{H}]^-$  of **1** at  $m/z$  269, (c)  $[M + \text{Li} + \text{NBA} - 2\text{H}]^-$  of **1** at  $m/z$  268, (d)  $[M + \text{Li} + \text{NBA} - 2\text{H}]^-$  of **3** at  $m/z$  268, (e)  $[M + \text{Li} + \text{NBA} - 2\text{H}]^-$  of **2** at  $m/z$  268, (f)  $[\text{Md}_2 + \text{Li} + \text{NBA}d_1 - \text{D}]^-$  of **1** at  $m/z$  271 and (g)  $[M + {}^6\text{Li} + \text{NBA} - \text{H}]^-$  of **1** at  $m/z$  268.

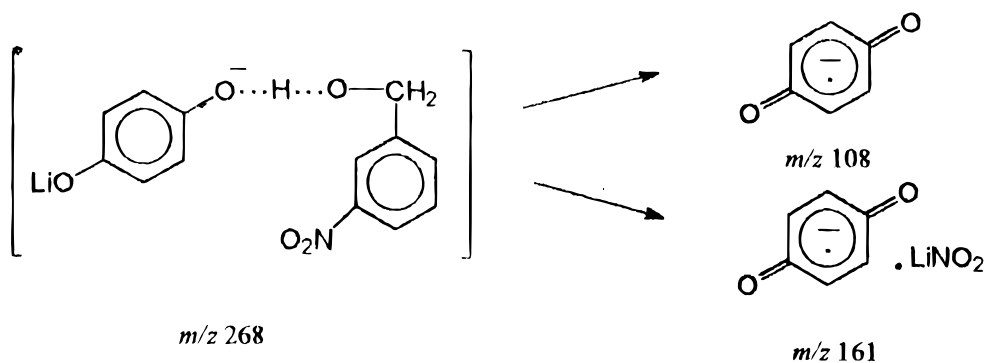




Scheme 4



Scheme 5



Scheme 6

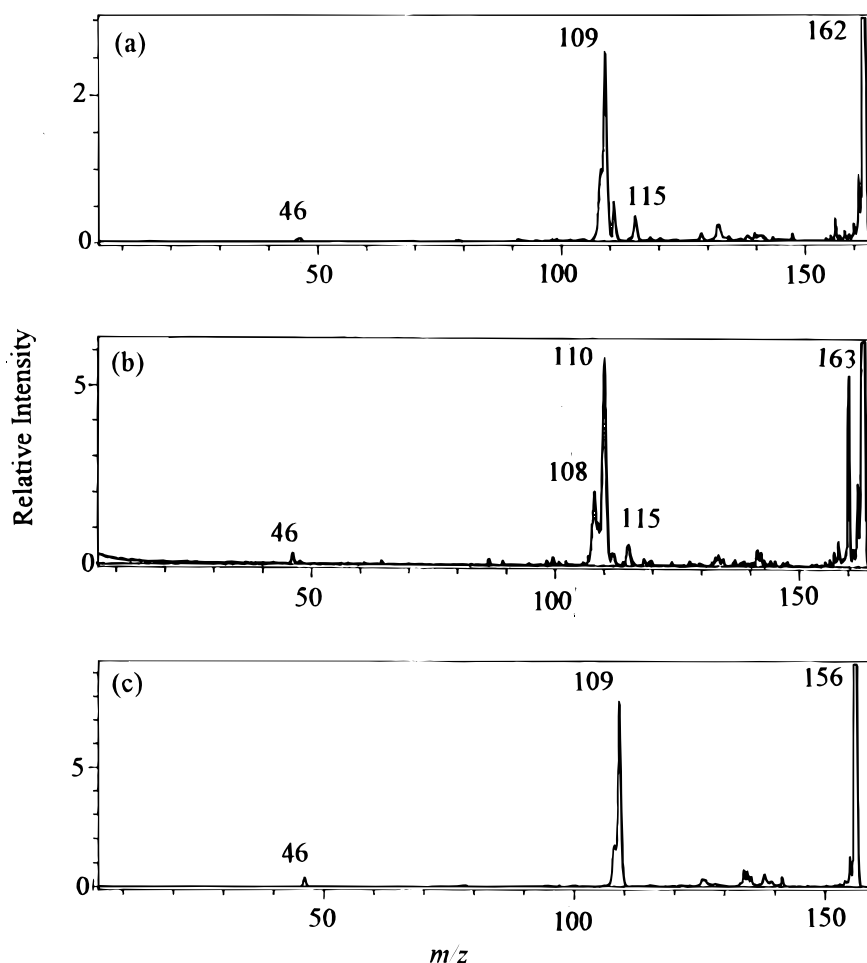


**Figure 5.** CID MIKE spectra of **1**: (a)  $[M + Li - H + NO_2]^-$  at  $m/z$  162, (b)  $[Md_2 + Li - D + NO_2]^-$  at  $m/z$  163 and (c)  $[M + NO_2]^-$  at  $m/z$  156.

## REFERENCES

1. K. P. Madhusudanan, *Rapid Commun. Mass Spectrom.* **11**, 295 (1997).
2. K. P. Madhusudanan, *J. Mass Spectrom.* **30**, 1230 (1995), and references cited therein.
3. K. P. Madhusudanan, *J. Mass Spectrom.* **30**, 639 (1995).
4. C.-G. Juo, L.-L. Shiu, C. K.-F. Shen, T.-Y. Luh and G.-R. Her, *Rapid Commun. Mass Spectrom.* **9**, 604 (1995).
5. D. J. Burinsky, E. K. Fukuda and J. E. Campana, *J. Amer. Chem. Soc.* **106**, 2770 (1984).
6. (a) G. Chen and R. G. Cooks, *J. Mass Spectrom.* **30**, 1167 (1995); (b) G. Chen, R. G. Cooks, E. Corpuz and L. T. Scott, *J. Am. Soc. Mass Spectrom.* **7**, 619 (1996).
7. V. A. Boote, J. M. Bruce, S. A. Clark, A. P. Pritchard and R. J. Speak, *Rapid Commun. Mass Spectrom.* **11**, 749 (1997).
8. (a) G. B. Anderson, R. G. Gillis, R. B. Johns, Q. N. Porter and M. G. Strachan, *Org. Mass Spectrom.* **19**, 199 (1984); (b) M. G. Strachan, G. B. Anderson, Q. N. Porter and R. B. Johns, *Org. Mass Spectrom.* **22**, 670 (1987); (c) G. B. Anderson, R. B. Johns, Q. N. Porter and M. G. Strachan, *Org. Mass Spectrom.* **19**, 583 (1984); (d) R. W. Binkley, G. W. Dillow, T. W. Fletcher, W. Winnik and M. J. S. Tevesz, *Org. Mass Spectrom.* **29**, 491 (1994).
9. T. Heinis, S. Chowdhury, S. L. Scott and P. Kebarle, *J. Am. Chem. Soc.* **110**, 400 (1988).
10. S. A. McLuckey, D. Cameron and R. G. Cooks, *J. Am. Chem. Soc.* **103**, 1313 (1981).
11. J. E. Bartmess, *Mass Spectrom. Rev.* **8**, 297 (1989).
12. S. M. Musser and J. A. Kelley, *Org. Mass Spectrom.* **28**, 672 (1993).
13. (a) A. Wakisaka, Y. Akiyama, Y. Yamamoto, T. Engst, H. Takeo, F. Mizukami, K. Sakaguchi and H. Jones, *J. Chem. Soc., Faraday Trans.* **92**, 3539 (1996); (b) T. Koyama and A. Wakisaka, *J. Chem. Soc., Faraday Trans.* in press.
14. X. Li and E. de Hoffmann, *J. Am. Soc. Mass Spectrom.* **6**, 1252 (1995).
15. F. W. Rollgen, F. Borchers, U. Geissmann and K. Levsen, *Org. Mass Spectrom.* **12**, 541 (1977).
16. K. P. Madhusudanan, L. K. Bajpai and A. P. Bhaduri, *Rapid Commun. Mass Spectrom.* **11**, 1263 (1997).